

Article

Evaluation of the Antifungal Activity of Gold–Chitosan and Carbon Nanoparticles on *Fusarium oxysporum*

Florin-Daniel Lipșa ¹ , Elena-Laura Ursu ², Cristian Ursu ³, Eugen Ulea ¹ and Ana Cazacu ^{4,*} 

¹ Department of Plant Sciences, “Ion Ionescu de la Brad” University of Agricultural Sciences and Veterinary Medicine, 3 Mihail Sadoveanu Alley, 700490 Iasi, Romania; flipsa@uaiasi.ro (F.-D.L.); eulea@uaiasi.ro (E.U.)

² Centre of Advanced Research in Bionanoconjugates and Biopolymers, “Petru Poni” Institute of Macromolecular Chemistry, 41A Grigore Ghica Voda Alley, 700487 Iasi, Romania; ursu.laura@icmpp.ro

³ Laboratory of Polymeric Materials Physics, “Petru Poni” Institute of Macromolecular Chemistry, 41A Grigore Ghica Voda Alley, 700487 Iasi, Romania; cristian.ursu@icmpp.ro

⁴ Department of Exact Sciences, “Ion Ionescu de la Brad” University of Agricultural Sciences and Veterinary Medicine, 3 Mihail Sadoveanu Alley, 700490 Iasi, Romania

* Correspondence: anacazacu@uaiasi.ro

Received: 27 June 2020; Accepted: 4 August 2020; Published: 6 August 2020



Abstract: Nanoparticles are implemented in different biotechnological fields, and there is interest in their use in plant biology. Nanotechnology can help overcome the persistent limitations of using conventional fungicides in the management of plant diseases, contributing to a safer environment. Hence, this study is focused on evaluating the behavior of nanoparticles on two different strains of *Fusarium oxysporum*, which have a wide-ranging occurrence in tomato production and account for important economic losses. *Fusarium oxysporum* is an ascomycetous fungus that is well-known as a soilborne plant pathogen, adapted to any soil type, and it lives in different forms on organic materials. Gold–chitosan and carbon nanoparticles were suspended in potato dextrose agar growth media, and their antifungal activity was evaluated at 1, 3, 5, and 7 days after incubation by measuring the diameter of fungal colonies. The results showed that the nanoparticles have antifungal properties against *F. oxysporum*, the fungal colony growth diameter being reduced. Likewise, it was observed that the colony diameter was smaller when the nanoparticle concentration increased. However, in the case of one *F. oxysporum* strain, the highest nanoparticle concentration applied during the experiment’s execution was not able to completely inhibit fungal growth.

Keywords: gold–chitosan nanoparticles; carbon nanoparticles; antifungal activity; *Fusarium oxysporum*

1. Introduction

In the domain of plant biology, temperature and humidity play important roles during the growth of the plants in the field as to fungal development and production of mycotoxins [1,2]. Fungi can affect and deteriorate plants throughout all of their phenophases or after harvesting, where the germination capacity of seeds is lost or the nutritional value of the plant products is reduced. The genus *Fusarium* includes major pathogens that can affect plant growth and development in the field, and since it develops resistance against conventional fungicides, new antifungal substances to control and inhibit fungal growth need to be produced. An interesting category of materials is those that present antifungal activity, which can also act as biostimulants, enabling plants to grow (through various processes) when used in small quantities. A special category of biostimulants is represented by nanoparticles (NPs), which have a high density of surface charges that interact with the surface charges found on cell walls and membranes [3]. Furthermore, NPs have started to be used as new types of agents with antimicrobial activity due to the wide possibilities of changing the combination of their physical and

chemical characteristics. The antimicrobial activity of NPs is associated with their interaction with the functional groups found on the surface of the microorganism's cells, leading to the microorganism's inactivation [4,5]. Among the studies regarding the effects of different metallic NPs on microorganisms, only a few are related to the influence of gold or carbon nanoparticles on bacteria [6] or fungi [7]. NPs can be produced by several methods, which include chemical reduction, sol-gel techniques, gas condensation, electrodeposition or vacuum deposition and vaporization, and pulsed laser ablation in liquid (PLAL). The chemical reduction method involves using a reducing agent (e.g., sodium borohydride, ascorbic acid, sodium citrate, amino acids) to obtain NPs from a bulk solution. PLAL is a versatile approach used for the synthesis of surfactant-free stable colloidal solutions of nanoparticles belonging to a wide range of materials [8]. For this study, two types of nanoparticles were synthesized: gold nanoparticles, by using chitosan (AuNPs–chitosan) that acts as both reducing and stabilizing agents, and carbon nanoparticles (CNPs), by using PLAL. Unlike other inorganic nanoparticles, gold NPs are known to be nontoxic due to their inert nature [9].

Owing to their many attractive properties, research on the quality improvement of carbon nanomaterials is of increasing interest [10,11], aiming to facilitate their use in various applications [12–14] such as plant science, drug delivery systems, energy storage devices, bioimaging, and biosensors. There are many types of carbon nanomaterials (e.g., carbon nanotubes, carbon nanoparticles, carbon dots) and, although they present a series of advantages, their potential toxicity to the environment is an important aspect that must be taken into account [15]. Nevertheless, depending on the experimental protocol used to manufacture them, some carbon nanomaterials may exhibit toxic effects while others may not [16]. Therefore, new ways of producing nontoxic carbon nanoparticles are being pursued, with the aim of safely using them for crop production enhancement [17].

The purpose of this study is to synthesize AuNPs–chitosan and CNPs and to evaluate their fungicidal activity on *F. oxysporum*.

2. Materials and Methods

All the materials used in the synthesis process of NPs were purchased from Sigma Aldrich and used without further purification.

2.1. Synthesis of Chitosan–Stabilized Gold Nanoparticles

To synthesize AuNPs–chitosan with concentrations of 25, 50, and 75 µg/mL, solutions of tetrachloroauric acid (HAuCl₄; 0.01 M) and 0.1 mg/mL chitosan were mixed in different ratios and then treated with an ultrasonic field (ultrasonic frequency of 45kHz; USC200TH-VWR ultrasonic unit) for 20 min at a temperature of 55 °C. AuNP formation in chitosan was demonstrated, at first, a few days later, by the color of the solution turning into shades of purple–pink (the initial solution being transparent). The intensity of the color increased along with the concentration of AuNPs. The samples were labeled based on the concentration of gold. For example, the sample of AuNPs–chitosan with a concentration of 25 µg/mL is referred to as AuNP25.

2.2. Synthesis of Carbon Nanoparticles

Stable CNP suspensions in ethanol were obtained by using the PLAL method, free of surfactants. A pyrolytic graphite disk (99.99% purity) immersed into 15 mL of ethanol (99.99%), with a liquid column height of 0.5 cm, was subjected to an Nd:YAG laser beam (1064 nm wavelength; 7 ns pulse duration) focused through a spherical lens with a focal length of 15 cm (Figure 1). A number of 18,000 pulses were used for the laser ablation of graphite, with a pulse repetition rate of 10 Hz. To ensure reproducibility of the experimental procedure used and an increased nanoparticle production rate, the laser spot was scanned along a helical trajectory through a continuous shift of its position on the target surface (in a radial direction from the disk center toward the edge) and simultaneous rotation of the target around its own axis. Hence, two solutions of CNPs were obtained for two laser

fluences values of 2 and 3 J/cm, resulting in the samples labeled as CNP_1 and CNP_2, respectively. The concentration for CNP_1 was 19 mg/mL and for CNP_2 was 23 mg/mL.

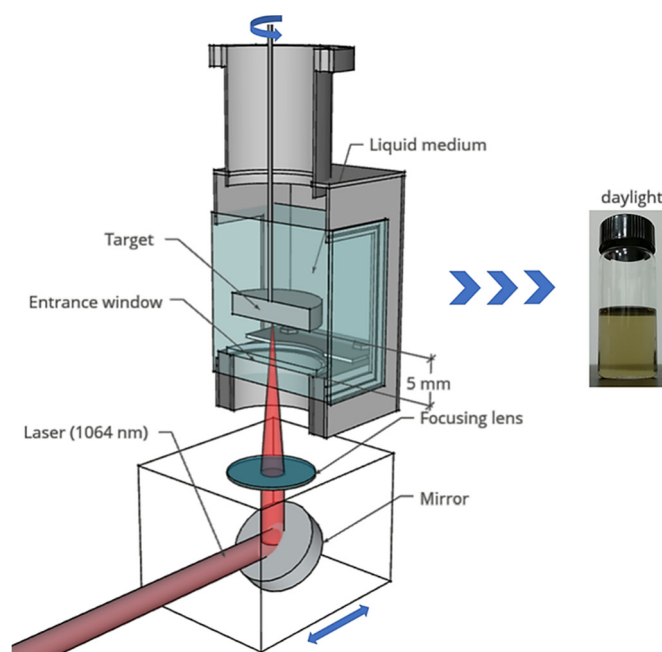


Figure 1. The experimental setup used for carbon nanoparticle (CNP) generation through the pulsed laser ablation in liquid (PLAL) method. The inset digital image shows the daylight appearance of the obtained CNP suspension in ethanol.

2.3. Characterization of Nanoparticles

UV–vis spectra were obtained with a Perkin Elmer Lambda 35 UV–vis spectrophotometer (200–700 nm wavelength range). Fluorescence measurements were carried out using a Fluoromax-4 Horiba spectrofluorometer. Dynamic light scattering (DLS) was used for the measurement of average particle size on a Delsa Nano C-Particle Analyzer (Beckman Coulter). The zeta potentials of the samples were evaluated using the same device for DLS measurements, which assesses the electrophoretic mobility of the particles and converts it to zeta potential using the von Smoluchowski equation. The results were expressed as the average values of three independent measurements performed for each sample. The atomic force microscopy (AFM) measurements were performed using an NT-MDT Ntegra Spectra instrument operated in tapping mode under ambient conditions. Silicon cantilever tips (NSG 10) with a resonance frequency of 140–390 kHz, a force constant of 5.5–22.5 N/m, and tip curvature radius of 10 nm were used. To prepare the samples for AFM measurements, 10 μ L of nanoparticle suspension was deposited on freshly cleaved mica substrates and air-dried at room temperature.

2.4. Nanoparticles Application to Fungi

The *F. oxysporum* strains DSM 62338 and DSM 62060 used in this study were acquired from the Leibniz Institute German Collection of Microorganisms and Cell Cultures (Deutsche Sammlung von Mikroorganismen und Zellkulturen (DSMZ)). The phytopathogenic fungi were routinely grown on potato dextrose agar (PDA) medium containing an infusion from 200 g potatoes, 20 g glucose, and 15 g agar (Merck, Germany) at 25 °C in the climatic chamber.

The antifungal properties of AuNPs–chitosan and CNPs against *F. oxysporum* strains were investigated at various concentrations, ranging from 25 to 75 μ g/mL in the case of AuNPs–chitosan and 19 to 23 mg/mL in the case of CNPs, respectively.

The two types of NPs (based on gold or carbon) were suspended in 15 mL PDA medium and poured into Petri dishes of 90 mm in diameter. The NP solutions were added in varying doses (0,

0.5, 1, 2, and 5 mL) into Petri dishes, with the purpose of finding the most efficient dose for each NP solution used (regardless of the initial concentration of the respective solution). The PDA medium was prepared and poured using the media preparator with automatic dispenser (Masterclave 09 + APS 320/90 AES Laboratoire, France) for Petri plates.

After cooling and solidification, the plates, supplemented with different concentrations of NPs, were inoculated aseptically with 7 mm diameter disks of *F. oxysporum* taken from an actively growing edge of a five-day-old culture and incubated at 28 °C for one week.

The mycelial growth was photographically recorded, and the fungal plaque diameter from the inoculated plates was measured every 24 h. The experiment was conducted with a threefold repetition for each microbiological determination. The obtained values were compared with that of the control (without NPs) in order to calculate the percentage of growth inhibition according to Formula (1):

$$\% \text{ Inhibition rate} = \frac{(M_c - M_t)}{M_c} \times 100, \quad (1)$$

where M_c is the mycelial growth for the control plate, and M_t is the mycelial growth for the plates treated with different dosage of NP solutions. Values are shown in terms of mean and standard deviation (mm).

2.5. Statistical Analysis

To evaluate the influence of nanoparticles on *F. oxysporum* strains, a two-sample t-test assuming unequal variances was carried out using Microsoft Excel 2016 software (Microsoft, USA). The values were compared with the average of all the values in the experiment (for each strain), and the differences were considered statistically significant at the 0.05 probability level ($p < 0.05$).

3. Results and Discussion

3.1. Synthesis and Characterization of Nanoparticles

To the best of our knowledge, chitosan was previously used to obtain gold nanoparticles at high temperatures or in the presence of additional reducing agents due to its low reducing ability [18,19]. Herein, we report a new mild and facile one-pot synthesis method for obtaining gold nanoparticles by exploiting the characteristics of chitosan, which acts as both reducing agent and stabilizer. The mechanism for the formation of gold nanoparticles involves three steps: (i) the binding of the metal salt anions (AuCl_4^-) to the protonated amino groups ($-\text{NH}_2$) at the C-2 position in chitosan due to the electrostatic attractive forces; (ii) the simultaneous reduction of Au^{3+} ions with the oxidation of the ($-\text{CH}_2\text{OH}$) groups at the C-6 position and ($-\text{CHO}$) groups at the C-1 position; (iii) the agglomeration of the reduced Au atoms and formation of gold nanoparticles that are further stabilized by chitosan [20–22]. Since chitosan is a natural polysaccharide with unique biological and physicochemical properties, its use in the synthesis process of gold nanoparticles hinders any environmental toxicity or biological hazards.

In order to confirm the formation of gold nanoparticles, a UV–visible analysis was performed. The obtained results show a UV–vis spectrum that consists of a single broad absorption band centered around the wavelength of 539 nm (Figure 2a), which is specific to gold nanoparticles [20,23]. Haiss et al. demonstrated that the optical properties of spherical gold nanoparticles are dependent on the particle size; hence, we can conclude that the AuNPs in chitosan have dimensions of about 60 nm [24].

The optical absorption band of CNPs was observed in the UV region, with a peak at the wavelength of 258 nm, and a tail extending into the visible range (see the black curve in Figure 2b). Fluorescence is one of the most important properties of CNPs from both the fundamental and application points of view, making them good candidates for use in bioimaging, sensors, and fluorescent inks [25]. Regardless of the laser fluence used, the synthesized CNPs in ethanol presented blue luminescence on exposure to UV light, as shown in the insets of Figure 2b,c. Upon excitation with a 340 nm light,

strong emission peaks located at 396 nm and 400 nm were observed for both CNP_1 and CNP_2 carbon suspensions synthesized at 2 and 3 J/cm, respectively. The obtained values for the absorption and photoluminescence (PL) bands are specific for the formation of CNPs.

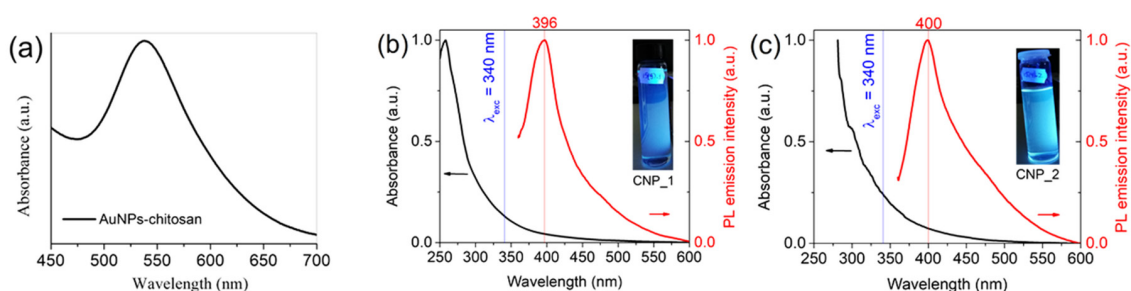


Figure 2. Optical properties of synthesized nanoparticles: (a) optical absorption spectrum of chitosan-stabilized gold nanoparticles (AuNPs–chitosan); (b) optical absorption and photoluminescence (PL) spectra of carbon nanoparticles (CNPs; excitation wavelength, $\lambda_{exc} = 340$ nm) obtained for a laser fluence of 2 J/cm (CNP_1) and (c) for a laser fluence of 3 J/cm (CNP_2). The inset photos in Figure 2b,c show the fluorescence of CNP suspensions taken under 365 nm UV light.

The increase of laser fluence leads to the formation of CNP suspensions in ethanol with a narrower PL spectrum that is red-shifted, the maximum PL emission changing from 396 nm (Figure 2b) to 400 nm (Figure 2c) for the same excitation wavelength of 340 nm. With laser fluence, an increase in the size of the obtained nanoparticles is expected, and the shift of the maximum PL emission towards shorter wavelengths confirms this behavior (Figure 2b,c). Additionally, the concentration of NPs increases and, hence, the scattering of light when passing through the solution is more significant, as reflected by an increase in the absorbance value at higher wavelengths (Figure 2c).

The surface morphological structure was further analyzed by AFM. The pure chitosan (Figure 3a) shows a granular structure, with grains having dimensions of about 29 nm. Comparing the results obtained for pure chitosan and AuNPs–chitosan (Figure 3a,b) it can be seen that the NPs are present as individual particles imbedded into chitosan aggregates (with a mean diameter of 80 nm). For CNPs, the AFM image indicates the presence of nanoparticles with diameters of about 23 nm.

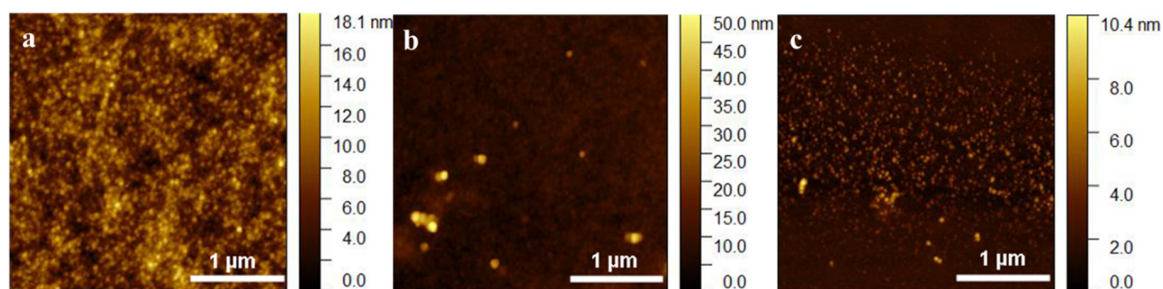


Figure 3. Atomic force microscopy (AFM) images of (a) pure chitosan, (b) gold–chitosan nanoparticles (AuNPs–chitosan), and (c) carbon nanoparticles (CNPs).

In order to characterize the stability of the obtained nanoparticles, the zeta potential of the solutions was measured (Figure 4a). Zeta potential is a physical parameter exhibited by any particle in suspension and it depends on the properties of both the particle surface and the surrounding liquid. The value of zeta potential is a degree of the electrostatic repulsion between charged particles in the dispersion. A high zeta-potential parameter involves a stronger repulsion between particles, which prevents aggregation, and the system is considered more stable. For AuNPs–chitosan, the obtained positive value of 42.17 mV is large enough to prevent particle agglomeration by electrostatic repulsion, thus confirming the stability of our colloidal dispersion. On the other hand, the CNPs have reached the upper limit of the light dispersion threshold (-22.96 mV) [26]. The DLS analysis of the CNPs indicates the presence of

a single population for both samples, with an average hydrodynamic diameter of 119.6 nm for CNP_1 and 96.8 nm for CNP_2 (Figure 4b).

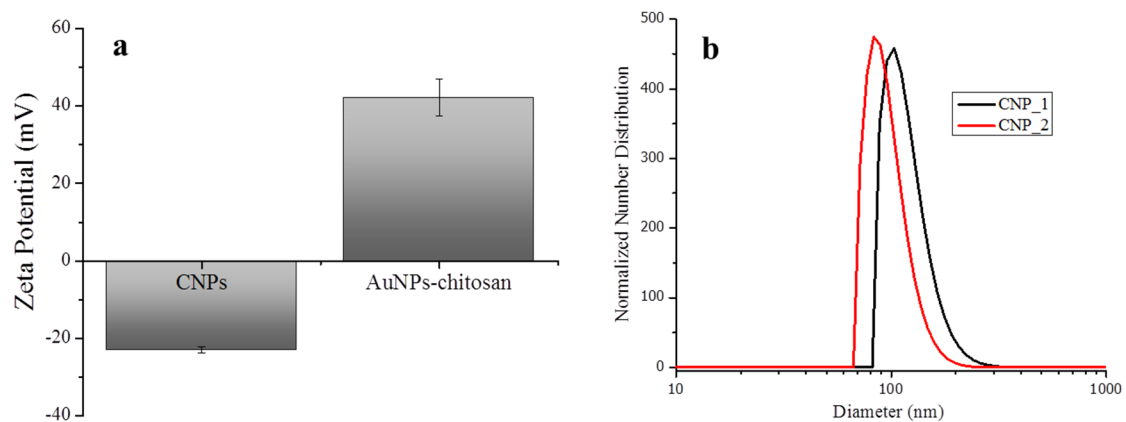


Figure 4. (a) Zeta potential for gold–chitosan (AuNPs–chitosan) and carbon nanoparticles (CNPs); (b) dynamic light scattering of the synthesized CNPs.

3.2. In Vitro Antifungal Assays

This study was conducted in order to determine the inhibitory activity of AuNPs–chitosan and CNPs on colony formation from the mycelia of *F. oxysporum* under laboratory conditions (in vitro). The growth rate of *F. oxysporum* strains in the presence of the tested NPs is presented in Figure 5.

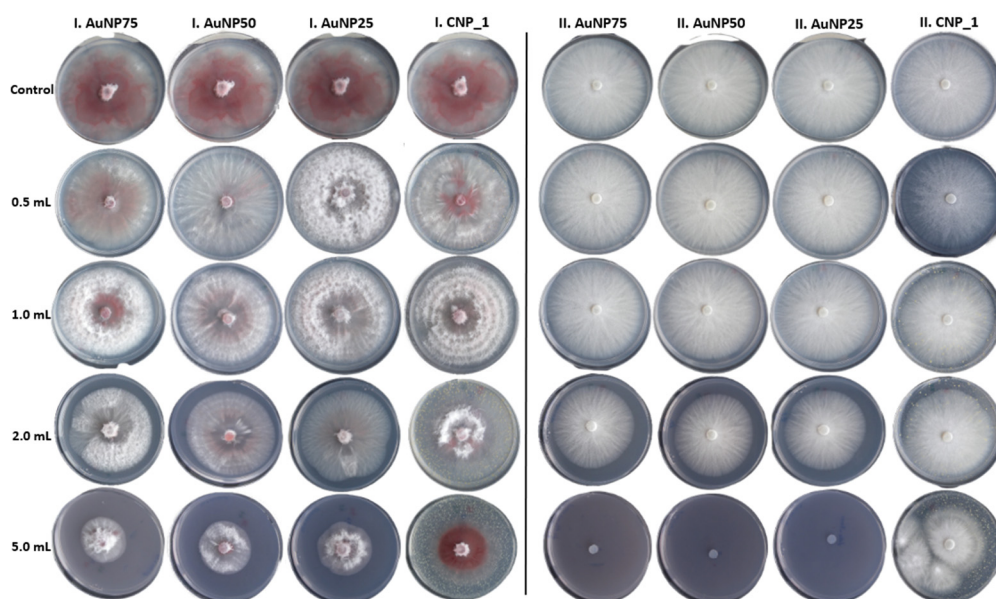


Figure 5. Effects of the interactions of different nanoparticles at different concentrations and doses on the inhibition of mycelial growth of two *F. oxysporum* strains. There was no inhibition in the case of the control plates. I—*F. oxysporum*, DSM 62338 strain; II—*F. oxysporum*, DSM 62060 strain. For all the controls, the same picture was used as there was no difference between the control plates.

The radial growth of *F. oxysporum* strains (DSM 62338 and DSM 62060) was differently inhibited by the tested NPs at different concentration levels. At the highest dosage used (5 mL), AuNPs–chitosan and CNPs (with the exception of CNP_2) showed inhibitory effects as compared to the lowest dosage (0.5 mL). The effect of AuNPs–chitosan and CNP concentrations on the mycelial growth of *F. oxysporum* strains tested after 7 days of incubation can be observed in Figures 5 and 6.

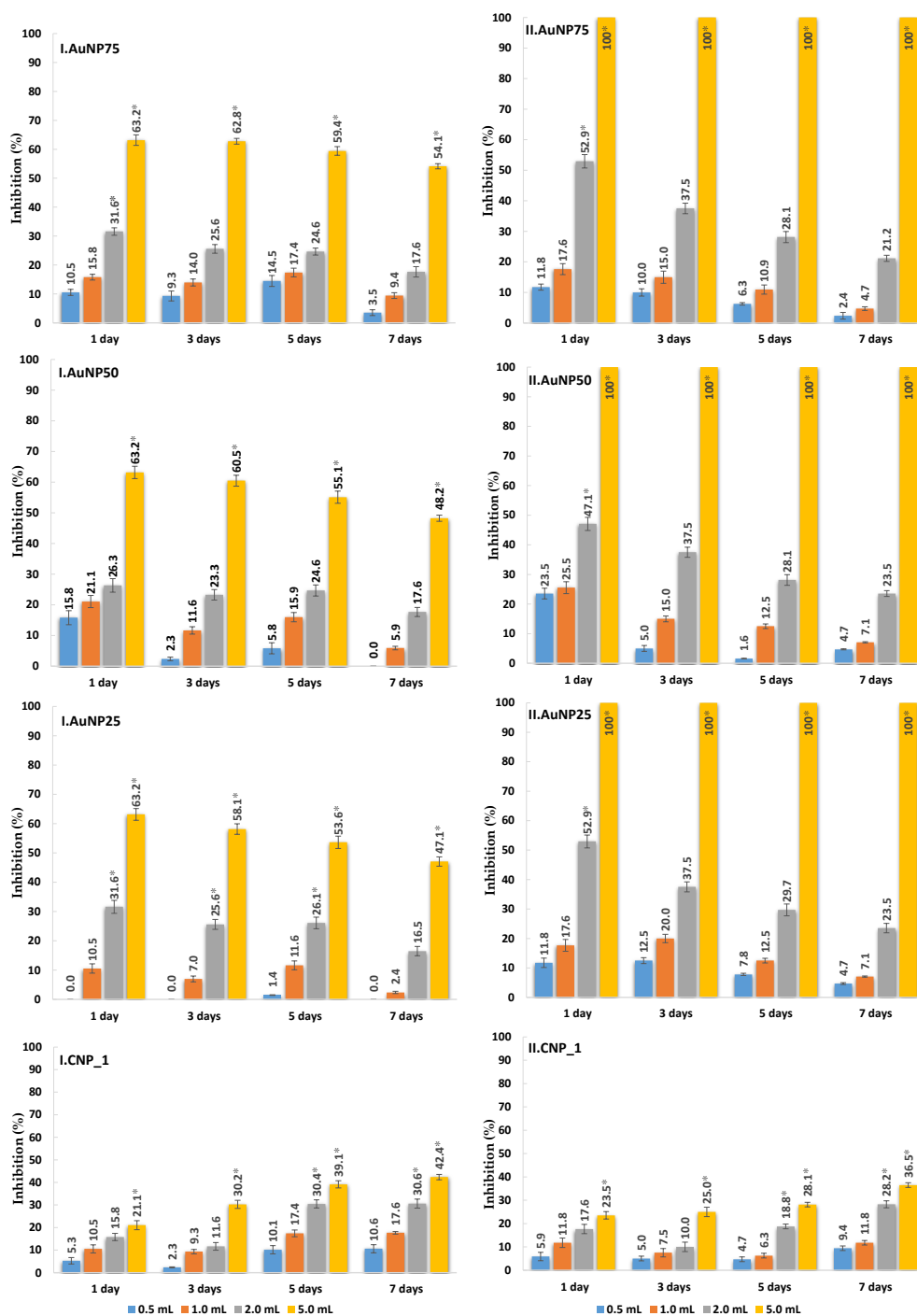


Figure 6. Antifungal activity of gold-chitosan (AuNPs-chitosan) and carbon nanoparticles (CNPs) applied at different concentrations and dosage on two *Fusarium oxysporum* strains grown on PDA medium after 1, 3, 5, and 7 days of incubation at 28 °C. *Fusarium oxysporum* strains DSM 62338 (I) and DSM 62060 (II) with different concentrations, ranging from 25 to 75 µg/mL in the case of AuNPs-chitosan and 19 mg/mL in case of CNPs. The percentages of growth inhibition were calculated in relation to the control. Error bars represent a standard deviation from the mean ($n = 3$). Significant differences ($p < 0.05$) are marked with an asterisk.

The application of AuNPs-chitosan at different concentrations and dosage was effective on both *F. oxysporum* strains; we have to mention, though, that in the case of the pathogen *F. oxysporum* DSM 62060 strain (II), a mycelial growth inhibition rate of 100% ($p < 0.05$) was observed. Absolute inhibitions

were obtained through the application of 5.0 mL AuNPs–chitosan for all three different concentrations (i.e., II.AuNP25, II.AuNP50, and II.AuNP75), the measurements being made after 1, 3, 5, and 7 days, respectively. On the other hand, in the case of the DSM 62338 strain (I), the application of the same dosage of AuNP25, AuNP50, and AuNP75 led to a good inhibition rate after 7 days of 47.1%, 48.2%, and 54.1%, respectively ($p < 0.05$).

In addition, in the case of lower concentrations and dosage for AuNPs–chitosan, a decrease of the mycelial growth inhibition was noted throughout the entire seven-day trial period. The results presented in Figure 6 showed that AuNP25 did not exhibit any antifungal activity in a dosage of 0.5 mL in the case of the DSM 62338 strain. In addition, it may be observed that the efficacy of all gold–chitosan nanoparticles increases with the dosage and concentration in almost all cases. The antifungal activity of AuNPs–chitosan against the plant pathogen might be attributed to a synergic effect between the gold nanoparticles and the chitosan.

These differences in the inhibition activity on *F. oxysporum* strains might be due to the presence of some different resistance tools against AuNPs–chitosan. Both strains were isolated from tomato plants (*Lycopersicon esculentum*), but their origin was different: the DSM 62060 strain originates from the USA, while the DSM 62338 strain comes from Italy. The differences we found in the percentage of inhibition are in agreement with the results published by Oh et al. (2019), who concluded that not all biological systems exhibit similar behavior under the influence of the same external agent [27]. For example, nanoparticles could reduce disease severity when used with a tolerant tomato cultivar, as previously reported by Bell et al. (1998) in the case of celery [28].

Gold nanoparticles exhibit a size-dependent antifungal activity against plasma membrane proteins [7]. NPs can interact directly with the enzymes involved in the regulation of the proton gradient across the plasma membrane and can cause activity loss. The fungal membrane would then be incapable of regulating the H^+ transport, leading to the retardation of cell growth and cell death [29]. According to another report, AuNPs may diffuse through the cell membrane and interact with the sulfur-containing proteins in the membrane or the phosphorus-containing bases in the DNA of the cells to inhibit synthesis, reparation, and replication, leading to the death of the cell [30].

Chitosan is one of the most promising products used against plant pathogens. Alone or in combination with other nanoparticles, it can improve antimicrobial activity by binding to the cell surface and inhibiting pathogen growth. The antimicrobial activity of chitosan is influenced by the type of chitosan, molecular weight, and concentration. Low molecular weight chitosan can pass through the fungal membrane and act against microbial development. At lower concentrations, chitosan binds to the cell surface of microorganisms and causes disruptions in the membrane, which eventually induces the death of the microbial cell by leakage of the intracellular components [31].

Regarding the efficacy of chitosan on *F. oxysporum*, Matei et al. (2018) presented some controversial results reported in the literature [32]. For example, Bell et al. (1998) studied the effect of chitosan on *F. oxysporum* in vivo and found that the incidence of the disease was not reduced by applying chitosan alone as a root dip; transplants treated with a solution of chitosan did not reduce soil populations of this plant pathogen either [28]. On the contrary, Al-Hetar et al. (2011) reported that different chitosan concentrations (0.5, 1, 2, 4, and 8 mg/mL) reduced the hyphal growth of *F. oxysporum* f. sp. *ubense*, reporting a maximum inhibition of 76.4% at 8 mg/mL [33].

Another part of our study consists of using CNPs at different concentrations (CNP_1—19 mg/mL, CNP_2—23 mg/mL) and doses (0.5, 1, 2, and 5 mL) to analyze the inhibitory effects on *F. oxysporum* strains DSM 62338 (I) and DSM 62060 (II).

The inhibitory effect of CNP_1 on both *F. oxysporum* strains was evident, especially for high dosage. From Figure 6, it can be observed that 7 days after inoculation and at the highest dosage (5 mL per Petri dish), maximum inhibition of 42.4% in the case of the DSM 62338 strain and 36.5% for the DSM 62060 strain was attained ($p < 0.05$). The lowest level of inhibition against both strains for CNP_1 was recorded at a dosage of 0.5 mL in nutritive media.

Similar to the AuNPs–chitosan effect, the measurements of mycelial growth during the entire period of experiments showed an increasing inhibitory effect of CNP_1 for all the doses used. Additionally, it may be observed that the inhibitory effect of CNP_1 is higher in the case of the DSM 62338 strain and lower in that of the DSM 62060 strain.

One possible mechanism of action for CNPs has been reported by Xie et al. (2016), who stated that CNPs could disturb fungal structures and damage the cell wall with their sharp edges, producing oxidative stress [34]. Another research study concluded that the antifungal mechanism of carbon nanomaterials is due to the inhibition of water uptake after their attachment to the surface of the spores, a phenomenon that induces plasmolysis [35].

In the case of CNP_2, in a higher concentration (since the initial concentration was 23 mg/mL) in comparison to CNP_1, despite the fact that the dimension of CNPs was smaller (CNP_2 = 97 nm vs. CNP_1 = 120 nm), the results showed no influence on the mycelia growth of CNP_2, regardless of the exposure doses, on both *F. oxysporum* strains assayed (data and figure not presented).

No inhibition on growth rates was registered for CNP_2 because the effects of CNPs within different biological systems (plants, microorganisms) are diverse and dependent on the CNP type, its physical characteristics, type of organism, dosage/concentration, method of application, and duration of the exposure. For plants, Verma reported all those effects. Verma et al. (2019) reported that at lower concentrations, CNPs were effective in enhancing water uptake and transport, seed germination, activating water channels proteins, and promoting the absorption of nutrients. When the CNP concentration was high, all these changes were not present anymore [36].

The results presented above for AuNPs–chitosan and CNP_1 revealed that statistically significant ($p < 0.05$) mycelial growth inhibition was observed in the case of both *F. oxysporum* strains. The greatest inhibition in the radial growth of the pathogen was noted for a 5-mL NP dosage, although significant differences were also found for a 2-mL dosage, especially in the case of CNP_1 (Figure 6).

4. Conclusions

The use of AuNPs–chitosan and CNPs in agricultural fields is a promising alternative technique to the traditional use of conventional fungicides for controlling plant pathogens such as *F. oxysporum*. The present study demonstrates that AuNPs–chitosan and CNP_1 have antifungal activity against two different strains of *F. oxysporum* that have a wide occurrence, affecting tomato production.

In the case of the *F. oxysporum* DSM 62060 strain, an absolute inhibition ($p < 0.05$) was obtained with the application of 5 mL of AuNPs–chitosan solution for all the concentrations used (25, 50, and 75 $\mu\text{g/mL}$). Our study proves that another factor to be considered when assessing the antifungal activity of an NP solution is the dose applied (regardless of the concentration used). Thus, instead of using an NP solution with a high concentration (implying higher production costs), a lower concentration solution can be used if the right dose to be applied is known.

In conclusion, particle size, molecular weight, concentration, and dosage are important factors that should be taken into account in the future preparation of new formulations of fungicides for applications in plant disease management. Therefore, more investigations on field applications (in vivo) are needed.

Author Contributions: Conceptualization, F.-D.L. and A.C.; methodology, F.-D.L., E.-L.U., C.U. and A.C.; formal analysis, F.-D.L., E.-L.U., C.U., E.U. and A.C.; investigation, F.-D.L., E.-L.U., C.U. and A.C.; writing—original draft preparation, F.-D.L., E.-L.U., C.U. and A.C.; writing—review and editing, F.-D.L., E.-L.U., C.U., E.U. and A.C.; supervision, A.C.; project administration, A.C.; funding acquisition, A.C. All authors have read and agreed to the published version of the manuscript.

Funding: This research was funded by the CNCS-UEFISCDI, PN-III-P1-1.1-TE-2016-2336 project.

Conflicts of Interest: The authors declare no conflict of interest. The funders had no role in the design of the study; in the collection, analyses, or interpretation of data; in the writing of the manuscript, or in the decision to publish the results.

References

1. Llorens, A.; Mateo, R.; Hinojo, M.J.; Valle-Algarra, F.M.; Jiménez, M. Influence of environmental factors on the biosynthesis of type B trichothecenes by isolates of *Fusarium* spp. from Spanish crops. *Int. J. Food Microbiol.* **2004**, *94*, 43–54. [[CrossRef](#)]
2. Mateo, J.J.; Mateo, R.; Jiménez, M. Accumulation of type A trichothecenes in maize, wheat and rice by *Fusarium sporotrichioides* isolates under diverse culture conditions. *Int. J. Food Microbiol.* **2002**, *72*, 115–123. [[CrossRef](#)]
3. Juárez-Maldonado, A.; Ortega-Ortíz, H.; Morales-Díaz, A.B.; González-Morales, S.; Morelos-Moreno, Á.; Cabrera-De la Fuente, M.; Sandoval-Rangel, A.; Cadenas-Pliego, G.; Benavides-Mendoza, A. Nanoparticles and nanomaterials as plant biostimulants. *Int. J. Mol. Sci.* **2019**, *20*, 162. [[CrossRef](#)]
4. Choi, O.; Deng, K.K.; Kim, N.-J.; Ross, L.; Surampalli, R.Y.; Hu, Z. The inhibitory effects of silver nanoparticles, silver ions, and silver chloride colloids on microbial growth. *Water Res.* **2008**, *42*, 3066–3074. [[CrossRef](#)] [[PubMed](#)]
5. Cui, Y.; Zhao, Y.; Tian, Y.; Zhang, W.; Lü, X.; Jiang, X. The molecular mechanism of action of bactericidal gold nanoparticles on *Escherichia coli*. *Biomaterials* **2012**, *33*, 2327–2333. [[CrossRef](#)]
6. Perni, S.; Piccirillo, C.; Pratten, J.; Prokopovich, P.; Chrzanowski, W.; Parkin, I.P.; Wilson, M. The antimicrobial properties of light-activated polymers containing methylene blue and gold nanoparticles. *Biomaterials* **2009**, *30*, 89–93. [[CrossRef](#)]
7. Ahmad, T.; Wani, I.A.; Lone, I.H.; Ganguly, A.; Manzoor, N.; Ahmad, A.; Ahmed, J.; Al-Shihri, A.S. Antifungal activity of gold nanoparticles prepared by solvothermal method. *Mater. Res. Bull.* **2013**, *48*, 12–20. [[CrossRef](#)]
8. Zeng, H.; Du, X.-W.; Singh, S.C.; Kulinich, S.A.; Yang, S.; He, J.; Cai, W. Nanomaterials via laser ablation/irradiation in liquid: A review. *Adv. Funct. Mater.* **2012**, *22*, 1333–1353. [[CrossRef](#)]
9. Rahimi, H.; Roudbarmohammadi, S.; Delavari, H.H.; Roudbary, M. Antifungal effects of indolicidin-conjugated gold nanoparticles against fluconazole-resistant strains of *Candida albicans* isolated from patients with burn infection. *Int. J. Nanomedicine* **2019**, *14*, 5323–5338. [[CrossRef](#)]
10. Ursu, C.; Nica, P.; Focsa, C. Excimer laser ablation of graphite: The enhancement of carbon dimer formation. *Appl. Surf. Sci.* **2018**, *456*, 717–725. [[CrossRef](#)]
11. Ursu, C.; Nica, P.; Rusu, B.G.; Focsa, C. V-shape plasma generated by excimer laser ablation of graphite in argon: Spectroscopic investigations. *Spectrochim. Acta Part B At. Spectrosc.* **2020**, *163*, 105743. [[CrossRef](#)]
12. Walkey, C.; Sykes, E.A.; Chan, W.C.W. Application of semiconductor and metal nanostructures in biology and medicine. *Hematology* **2009**, *2009*, 701–707. [[CrossRef](#)] [[PubMed](#)]
13. Chung, H.; Son, Y.; Yoon, T.K.; Kim, S.; Kim, W. The effect of multi-walled carbon nanotubes on soil microbial activity. *Ecotoxicol. Environ. Saf.* **2011**, *74*, 569–575. [[CrossRef](#)]
14. Baughman, R.H.; Zakhidov, A.A.; Heer, W.A. de Carbon nanotubes—the route toward applications. *Science* **2002**, *297*, 787–792. [[CrossRef](#)] [[PubMed](#)]
15. Poland, C.A.; Duffin, R.; Kinloch, I.; Maynard, A.; Wallace, W.A.H.; Seaton, A.; Stone, V.; Brown, S.; MacNee, W.; Donaldson, K. Carbon nanotubes introduced into the abdominal cavity of mice show asbestos-like pathogenicity in a pilot study. *Nat. Nanotechnol.* **2008**, *3*, 423–428. [[CrossRef](#)] [[PubMed](#)]
16. Firme, C.P.; Bandaru, P.R. Toxicity issues in the application of carbon nanotubes to biological systems. *Nanomed. Nanotechnol. Biol. Med.* **2010**, *6*, 245–256. [[CrossRef](#)]
17. Zaytseva, O.; Neumann, G. Carbon nanomaterials: Production, impact on plant development, agricultural and environmental applications. *Chem. Biol. Technol. Agric.* **2016**, *3*, 17. [[CrossRef](#)]
18. Wang, B.; Chen, K.; Jiang, S.; Reincke, F.; Tong, W.; Wang, D.; Gao, C. Chitosan-mediated synthesis of gold nanoparticles on patterned poly (dimethylsiloxane) surfaces. *Biomacromolecules* **2006**, *7*, 1203–1209. [[CrossRef](#)]
19. Esumi, K.; Takei, N.; Yoshimura, T. Antioxidant-potentiality of gold–chitosan nanocomposites. *Colloids Surf. B Biointerfaces* **2003**, *32*, 117–123. [[CrossRef](#)]
20. Sun, L.; Li, J.; Cai, J.; Zhong, L.; Ren, G.; Ma, Q. One pot synthesis of gold nanoparticles using chitosan with varying degree of deacetylation and molecular weight. *Carbohydr. Polym.* **2017**, *178*, 105–114. [[CrossRef](#)]
21. Huang, H.; Yang, X. Synthesis of chitosan-stabilized gold nanoparticles in the absence/presence of tripolyphosphate. *Biomacromolecules* **2004**, *5*, 2340–2346. [[CrossRef](#)] [[PubMed](#)]

22. Guibal, E. Heterogeneous catalysis on chitosan-based materials: A review. *Prog. Polym. Sci.* **2005**, *30*, 71–109. [[CrossRef](#)]
23. Zuber, A.; Purdey, M.; Schartner, E.; Forbes, C.; van der Hoek, B.; Giles, D.; Abell, A.; Monro, T.; Ebendorff-Heidepriem, H. Detection of gold nanoparticles with different sizes using absorption and fluorescence based method. *Sens. Actuators B Chem.* **2016**, *227*, 117–127. [[CrossRef](#)]
24. Haiss, W.; Thanh, N.T.K.; Aveyard, J.; Fernig, D.G. Determination of size and concentration of gold nanoparticles from UV–Vis spectra. *Anal. Chem.* **2007**, *79*, 4215–4221. [[CrossRef](#)]
25. Yu, C.; Xuan, T.; Yan, D.; Lou, S.; Hou, X.; Chen, Y.; Wang, J.; Li, H. Sesame-derived ions co-doped fluorescent carbon nanoparticles for bio-imaging, sensing and patterning applications. *Sens. Actuators B Chem.* **2017**, *253*, 900–910. [[CrossRef](#)]
26. Control of Colloid Stability through Zeta Potential & its Relationship to Cardiovascular Disease. Available online: <http://customers.hbci.com/~{}wenonah/riddick/index.html> (accessed on 25 June 2020).
27. Oh, J.-W.; Chun, S.C.; Chandrasekaran, M. Preparation and *in vitro* characterization of chitosan nanoparticles and their broad-spectrum antifungal action compared to antibacterial activities against phytopathogens of tomato. *Agronomy* **2019**, *9*, 21. [[CrossRef](#)]
28. Bell, A.A.; Hubbard, J.C.; Liu, L.; Davis, R.M.; Subbarao, K.V. Effects of chitin and chitosan on the incidence and severity of Fusarium yellows of celery. *Plant Dis.* **1998**, *82*, 322–328. [[CrossRef](#)]
29. Beyenbach, K.W.; Wiczeorek, H. The V-type H⁺ ATPase: Molecular structure and function, physiological roles and regulation. *J. Exp. Biol.* **2006**, *209*, 577–589. [[CrossRef](#)]
30. Tan, Y.N.; Lee, K.H.; Su, X. Study of single-stranded DNA binding protein–nucleic acids interactions using unmodified gold nanoparticles and its application for detection of single nucleotide polymorphisms. *Anal. Chem.* **2011**, *83*, 4251–4257. [[CrossRef](#)]
31. Hosseinnejad, M.; Jafari, S.M. Evaluation of different factors affecting antimicrobial properties of chitosan. *Int. J. Biol. Macromol.* **2016**, *85*, 467–475. [[CrossRef](#)]
32. Matei, P.M.; Iacomi, B.M.; Martín-Gil, J.; Pérez-Lebeña, E.; Ramos-Sánchez, M.C.; Barrio-Arredondo, M.T.; Martín-Ramos, P. *In vitro* antifungal activity of composites of AgNPs and polyphenol inclusion compounds against *Fusarium culmorum* in different dispersion media. *Agronomy* **2018**, *8*, 239. [[CrossRef](#)]
33. Al-Hetar, M.Y.; Abidin, M.A.Z.; Sariah, M.; Wong, M.Y. Antifungal activity of chitosan against *Fusarium oxysporum* f. sp. *ubense*. *J. Appl. Polym. Sci.* **2011**, *120*, 2434–2439. [[CrossRef](#)]
34. Xie, J.; Ming, Z.; Li, H.; Yang, H.; Yu, B.; Wu, R.; Liu, X.; Bai, Y.; Yang, S.-T. Toxicity of graphene oxide to white rot fungus *Phanerochaete chrysosporium*. *Chemosphere* **2016**, *151*, 324–331. [[CrossRef](#)] [[PubMed](#)]
35. Wang, X.; Liu, X.; Chen, J.; Han, H.; Yuan, Z. Evaluation and mechanism of antifungal effects of carbon nanomaterials in controlling plant fungal pathogen. *Carbon* **2014**, *68*, 798–806. [[CrossRef](#)]
36. Verma, S.K.; Das, A.K.; Gantait, S.; Kumar, V.; Gurel, E. Applications of carbon nanomaterials in the plant system: A perspective view on the pros and cons. *Sci. Total Environ.* **2019**, *667*, 485–499. [[CrossRef](#)]

